

Strong Light–Matter Interactions between Gap Plasmons and Two-Dimensional Excitons under Ambient Conditions in a Deterministic Way

Longlong Yang, Xin Xie, Jingnan Yang, Mengfei Xue, Shiyao Wu, Shan Xiao, Feilong Song, Jianchen Dang, Sibai Sun, Zhanchun Zuo, Jianing Chen,* Yuan Huang,* Xingjiang Zhou, Kuijuan Jin, Can Wang,* and Xiulai Xu*



Cite This: *Nano Lett.* 2022, 22, 2177–2186



Read Online

ACCESS |



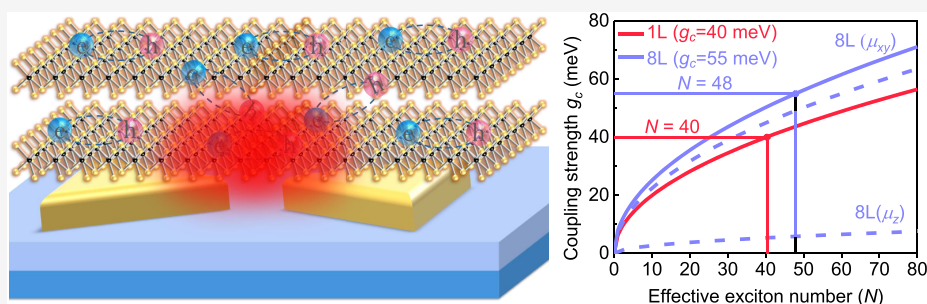
Metrics & More



Article Recommendations



Supporting Information



ABSTRACT: Strong exciton–plasmon interactions between layered two-dimensional (2D) semiconductors and gap plasmons show a great potential to implement cavity quantum electrodynamics under ambient conditions. However, achieving a robust plasmon–exciton coupling with nanocavities is still very challenging, because the layer area is usually small in the conventional approaches. Here, we report on a robust strong exciton–plasmon coupling between the gap mode of a bowtie and the excitons in MoS₂ layers with gold-assisted mechanical exfoliation and nondestructive wet transfer techniques for a large-area layer. Due to the ultrasmall mode volume and strong in-plane field, the estimated effective exciton number contributing to the coupling is largely reduced. With a corrected exciton transition dipole moment, the exciton numbers are extracted as being 40 for the case of a single layer and 48 for eight layers. Our work paves the way to realize strong coupling with 2D materials with a small number of excitons at room temperature.

KEYWORDS: strong coupling, transition-metal dichalcogenides, exciton, gap plasmon, effective exciton number

INTRODUCTION

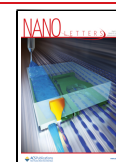
Atomically thin transition-metal dichalcogenides (TMDs) have been exploited widely for numerous optoelectronic and photonic applications, including single-photon emitters,^{1,2} transistors,^{3,4} photodetectors,^{5,6} and valleytronic devices.^{7,8} One of the intriguing properties is the large exciton binding energy,^{9,10} providing the opportunity to study the interaction of light and matter at room temperature when these TMDs are embedded in a microcavity.^{11,12} When the rate of coherent energy transfer between an excitonic transition and photons in a cavity is faster than their average dissipation rate, the system goes into a strong coupling regime, resulting in the formation of part-light and part-matter bosonic quasiparticles called microcavity polaritons.^{13,14} Polaritons in microcavities provide excellent platforms to realize Bose–Einstein condensation,^{15,16} low-threshold lasing,^{17,18} low-energy switching,^{19,20} and quantum information processing.^{21,22}

In order to achieve strong coupling with excitons in TMDs, optical cavities such as Fabry–Pèrot cavities and photonic crystal microcavities^{23,24} have been employed widely at cryogenic temperatures and under high vacuum.^{25,26} Even though a few of them have been used to demonstrate strong coupling at room temperature,^{13,27,28} the Rabi splittings are on the order of thermal energy $k_B T$ (~ 26 meV).^{29,30} Plasmonic nanocavities such as individual metallic nanoparticles³¹ or dimers³² can provide surface plasmon polaritons (SPPs) with light confined at the subwavelength scale, which is an alternative choice for realizing strong coupling under ambient

Received: August 24, 2021

Revised: February 24, 2022

Published: March 3, 2022



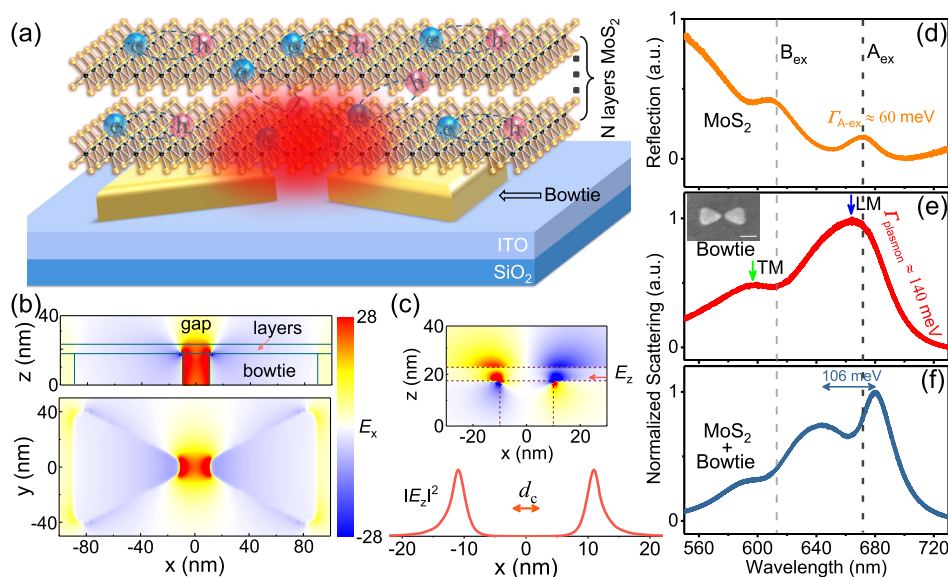


Figure 1. TMDs excitons, gap plasmons, and strong coupling between them. (a) Schematic of the system with layered MoS₂ on a single gold bowtie resonator. (b) x component of electric fields viewed from the x - z (crosses along the middle line of the bowtie) and x - y (within the layers) planes corresponding to gap resonances. (c) (top) z component of electric fields viewed from the x - z plane. (bottom) Distribution of electric field intensity along the position indicated by the magenta arrow. The baseline of the lower curve is zero. (d) Reflection spectrum of eight-layer MoS₂ on an ITO/glass substrate, showing an A exciton peak with a line width of 60 meV. (e) Scattering spectrum of the bowtie resonator, showing a well-isolated longitudinal mode (LM) with a line width of about 140 meV and a transverse mode (TM). The inset shows a corresponding scanning electron microscopy (SEM) image of the bowtie nanostructure with a gap distance of ~ 20 nm (scale bar: 100 nm). (f) Scattering spectrum of a coupled hybrid system.

conditions: for example, a coupled system with nanoparticle and layered TMDs.^{29,33–36}

The plasmonic nanocavities with mode volumes beyond the diffraction limit make it possible to demonstrate strong coupling with a small number of excitons, which has rich applications in the research of quantum many-body phenomena,³⁷ a photon blockade with many emitters,³⁸ cavity cooling,³⁹ and so on. Recently, gap plasmon systems with ultimate field confinement have been used to realize strong coupling with single molecules³¹ and single quantum dots,³² indicating the potential for applications at the quantum optics level.^{40,41} For layered TMDs, particle-on-film systems with nanoparticles⁴² or single plasmonic structures such as nanorods,⁴³ nanodisks,⁴⁴ and nanocuboids⁴⁵ have been used to demonstrate strong coupling. However, drop-casted nanoparticles intrinsically induce randomness, which cannot guarantee the robustness and the reproducibility in a deterministic way. The robustness is very important in particular for a strong coupled system with a small number of excitons.^{46,47} In addition, the resonant optical field in such cavities is typically polarized perpendicularly to the layer planes when it is embedded with two-dimensional semiconductors,^{29,35} which impedes an efficient coupling with the exciton dipole oriented almost in-plane. Therefore, the precise engineering orientations of exciton dipole and cavity modes is highly desirable for large coupling strength with a small number of excitons.

To demonstrate the strong coupling in plasmon–exciton (“plexiton”) with a small number of excitons, an estimation of the exciton number is crucial. So far, exciton number extractions by different methods have shown a very large discrepancy.^{33,35,36,43,48,49} Experimentally, the exciton number evolved in a strongly coupled system is related to the coupling strength, mode volume, and the exciton transition dipole

moment of TMDs.³⁵ The coupling strength can be measured, and the mode volume can be calculated with a good accuracy. It has been noted that the exciton transition dipole moment causes the main difference in previous work, which has been calculated with a traditional quantum well recombination model⁵⁰ or extracted with absorption spectra.³³ Here, we verify the two methods and correct the transition dipole moment values for the estimation of the exciton number.

In this work, we report on an observation of robust, strong plasmon–exciton coupling between gap plasmons confined within individual gold bowties and excitons in MoS₂ layers under ambient conditions by utilizing a gold-assisted mechanical exfoliation method and wet transfer techniques. Due to the strong in-plane electric field inside the material and small mode volume introduced by the bowtie resonator, vacuum Rabi splittings of up to 110 and 80 meV are obtained for the coupling systems with eight-layer and single-layer MoS₂, respectively. The estimated effective exciton number N contributing to the coupling with the gap mode is reduced to $N \approx 40$ for the case of a single layer and $N \approx 48$ for the case of eight layers with a corrected dipole moment. The robust, strong plasmon–exciton coupling with a lower exciton number paves the way for future scalable integrated nanophotonic devices.

RESULTS AND DISCUSSION

Figure 1a shows a schematic diagram of the plasmon–exciton coupling system with layered MoS₂ on top of a bowtie nanostructure. Here, the gold bowtie is employed as a plasmonic nanocavity for two reasons. First, it provides an ultraconfined gap plasmon mode with a mode volume of around 10^3 nm^3 .^{32,51} More importantly, when the high-refractive-index MoS₂ layers are covered on the surface of a bowtie, the strongly confined in-plane electric component of

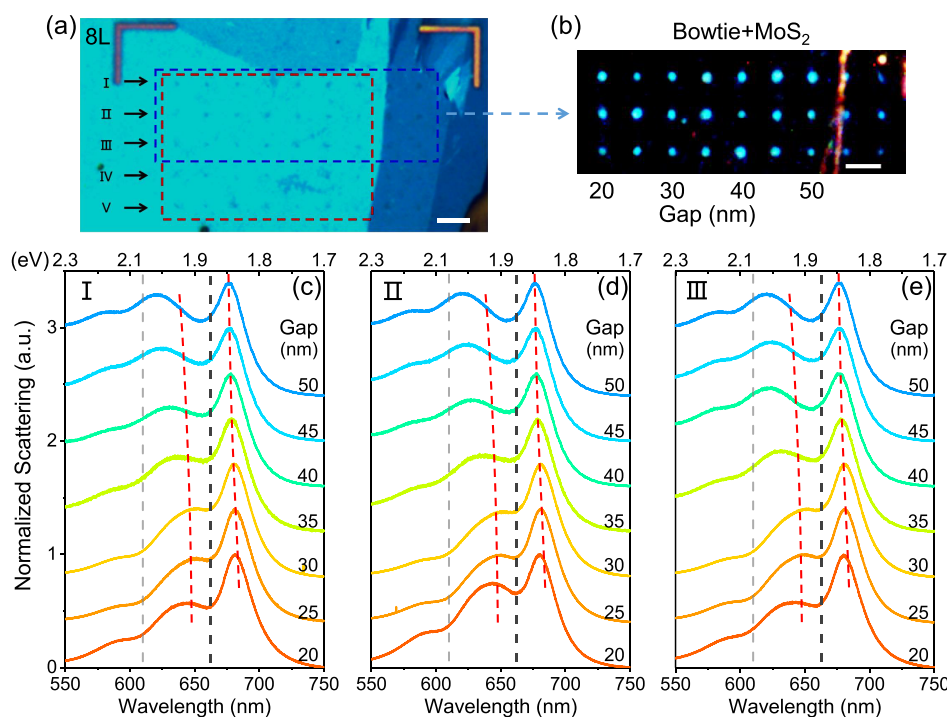


Figure 2. Strong coupling of individual bowtie resonators with eight-layer MoS₂. (a) Bright-field image of MoS₂ layers on bowties (scale bar: 4 μ m). The gap distance of the bowtie increases from left to right, and five rows of bowties with the same parameters are coated by MoS₂ layers (red dashed box). (b) Dark-field image of the first three rows in (a) (blue dashed box) (scale bar: 4 μ m). (c–e) DF scattering spectra of coupled hybrid systems at the first three rows. The dark dashed lines and gray dashed lines represent the absorption peak positions of A and B excitons, respectively. Red dashed curves trace (guide to the eye) the dispersion of plexciton branches.

the gap mode expands in the material (as shown Figure 1b), as calculated with the finite-difference time-domain method, indicating that the excitons above the gap will be strongly coupled to the gap mode. Normally in particle-on-film systems, the main electric field of the gap plasmon is dominated by an out-of-plane component (E_z)^{29,35} and strong coupling is achieved with the contribution of a large number of excitons. Our configuration is more suitable to enhance the coupling strength for the single-layer TMDs with a completely in-plane dipole orientation or a few layers with the in-plane dipole strength dominating.⁵²

To further compress the exciton number contributing to the plasmon–exciton interaction, a localized electric field region comparable to the effective exciton area is required. The excitons in TMDs are delocalized quasi-particles formed in semiconductor band gaps and extending much larger than a single unit cell⁵³ with an exciton coherence length d_c of ~ 4 nm for single-layer MoS₂ (Section III of the Supporting Information). Figure 1c shows the distribution of the out-of-plane component E_z of the gap mode. It can be seen that the electric fields between two tips have opposite phases but the intensities rapidly decay to zero inside the gap. Therefore, a gap distance slightly larger than the exciton coherence length should be able to couple the gap mode to a few excitons with a constructive interference. In our device, the bowtie nanocavity was designed with a gap distance of about 20 nm. The corresponding dark-field (DF) scattering spectrum (Figure 1e) shows a well-defined longitudinal gap mode at about 1.87 eV and a transverse mode at about 2.07 eV (Figure S7 in the Supporting Information). Clearly, the longitudinal gap mode overlaps with the emission peak of the A exciton of MoS₂ (Figure 1d), satisfying the requirement of spectral coincidence.

Furthermore, a stable and reproducible coupled system is important to achieve strong coupling especially at a few-exciton level, which has been an issue for systems based on colloidal quantum dots, molecules, and TMDs^{31,32,54,55} because of the randomness in exciton materials or plasmon nanocavities.⁵³ Here, we have made two efforts to address this problem. First, a contamination-free, one-step, and universal gold-assisted mechanical exfoliation method⁵⁶ has been used to obtain millimeter-size mono-/multilayer MoS₂ (see Section I of the Supporting Information for more details), on the basis of the covalent-like quasi bonding between the Au adhesion layer and the layered crystal. The quality of obtained MoS₂ layers is similar to that of the flakes prepared by traditional mechanical exfoliation, with clear Raman signals and photoluminescence from excitons (Figures S4 and S5 in the Supporting Information). This exfoliation method with high yield ratio and large-area layers is essential for the rest of the systematic studies. Second, to guarantee the stability of the coupled systems, a nondestructive wetting transfer method has been used to transfer thin layers to the prepared nanocavities, without damaging the fragile nanostructures during the transfer process (see Section I of the Supporting Information for more details). As a result, a splitting of about 106 meV is achieved in a coupled system with resonators combined with eight-layer MoS₂ (as shown in Figure 1f).

To verify that the coupled system is in the strong coupling regime, tuning the plasmon mode to cross the energy of an A exciton is required. In most cases, the tuning comes from randomly distributed nanoparticles with different sizes.^{31,34–36} Since the energy of a plasmon is sensitive to the particle size, this inevitably limits the reliability and repeatability of the system. Particularly for MoS₂, the splitting of spin–orbit

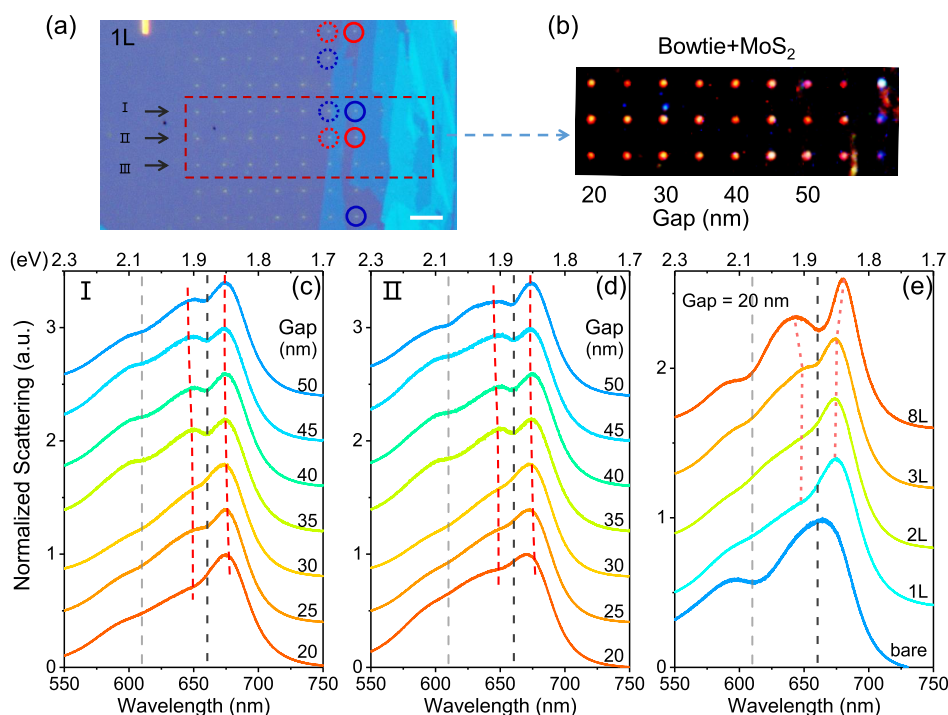


Figure 3. Exciton–plasmon coupling in different layers of MoS₂. (a) Bright-field image of single-layer MoS₂ on bowties. The parameters of bowties from left to right are the same as those in Figure 2. (b) The corresponding dark-field image in (a) (scale bar: 4 μ m). (c, d) DF scattering spectra of lines I and II, respectively. The spectra from devices marked with circles in I and II are replaced from other devices with the same circles covered with a single layer. The dark dashed lines and gray dashed lines represent the absorption peak positions of A and B excitons, respectively. Red dashed curves (guide to the eye) trace the dispersion of plexciton branches. (e) Scattering spectra of different layers of MoS₂ on bowties with the same gap distance of about 20 nm.

coupling is close to the value of Rabi splitting, complicating the study of such a system because of the emission of the B exciton. Here, increasing the gap distances of bowtie resonators has been used to tune gap modes in a way more moderate than tuning sizes (Figures S10 and S11 in the Supporting Information).

Figure 2a shows a bright-field image of the bowties covered with a large area of MoS₂ layers. It can be seen that the whole area is flat without any wrinkles due to the above exfoliation and transfer techniques. The smallest gap distances of bowties are 20 ± 2 nm and increase by approximately 5 nm for each step from left to right (Figures S1 and S2 in the Supporting Information). The red dashed box indicates that there are five rows of bowties covered well by flakes, labeled with Roman numerals from I to V. Figure 2b shows the dark-field image of the first three rows. The clear and bright spots of hybrid nanostructures indicate that the TMD layers are combined well with the plasmonic resonators without extra wrinkles and bubbles.

The normalized scattering spectra from rows I–III (Figure 2c–e) and IV and V (Figure S15 in the Supporting Information) all show similar behaviors, indicating a good robustness. When the gap distance is around 20 nm, an obvious double-peaked splitting around the position of the A exciton is observed, representing the energy of the upper plexciton branches (UPBs) and lower plexciton branches (LPBs). It is worth noting that the transferred MoS₂ layers will change the dielectric environment of resonators and result in a slight red shift of the plasmon mode due to the dielectric screening effect.^{33,57} With an increase in gap distance, the longitudinal mode continuously blue shifts and eventually

crosses the excitonic transition (see Section II of the Supporting Information for a discussion of energy tuning between an exciton and a plasmon). To extract the peak energies of UPBs and LPBs with the Lorentzian fitting method, we fix the resonance of the B exciton at about 2.0 eV according to the reflection spectrum in Figure 1d (see Figure S17 in the Supporting Information for fitting details). The red dashed curves in the scattering spectra trace the dispersion of plexciton branches, showing that the UPB is getting closer to the resonance of the B exciton as the gap increases but does not overlap with it, which means unambiguously here that the longitudinal plasmon mode only couples with the A exciton of MoS₂.

Similar splitting properties are also observed in the devices covered with a single layer. Figure 3a shows a bright-field image of the bowtie resonators with a large area of single-layer flake. The corresponding dark-field image is shown in Figure 3b, where the resonator parameters are the same as those above. Figure 3c,d shows the measured scattering spectra of lines I and II, respectively, with consistent spectral features (see Figure S16 in the Supporting Information for line III). It can be seen that a relatively small splitting is observed in comparison with that of eight layers. The splitting dependence on layer thickness has also been studied. As shown in Figure 3e, the magnitude of splitting in the spectra increases with the layer thickness with a gap distance of ~ 20 nm, implying an increase of coupling strength with the number of layers. Although strong coupling for all of the different layers has not been experimentally achieved, the splitting difference for different layers is obvious.

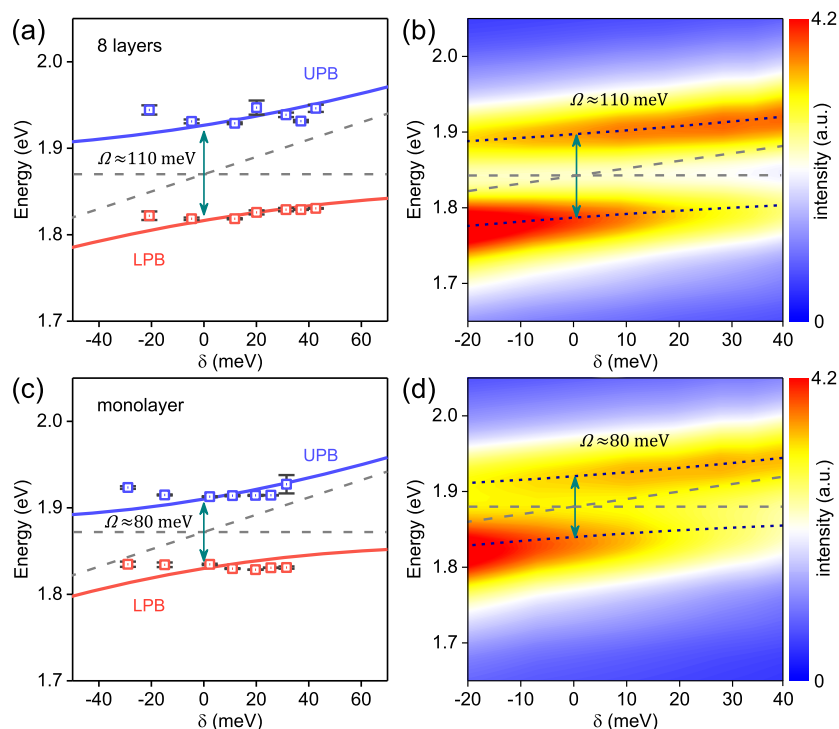


Figure 4. Dispersion of plexcitons and the corresponding calculation results. (a, c) Average energies of the UPBs (blue squares) and LPBs (magenta squares) of the several sets of data as a function of the detuning for the coupling with eight layers and a single layer, respectively. The curves in both (a) and (c) are fitted to the JC model (eq 1), giving Rabi splittings of 110 and 80 meV, respectively. (b, d) Calculated cross sections of individual bowtie resonators covered by eight-layer and single-layer MoS₂, respectively, as a function of the detuning. The exciton energy and plasmon energy are denoted by gray dashed lines.

The coupled system can be described by the simplified Jaynes–Cummings model (JC model) given by^{14,35,58}

$$\omega_{\pm} = \frac{1}{2}(\omega_{\text{pl}} + \omega_{\text{ex}}) \pm \sqrt{g_c^2 + \frac{1}{4}\delta^2} \quad (1)$$

where ω_{pl} and ω_{ex} are the energies of plasmons and excitons, respectively, $\delta = \omega_{\text{pl}} - \omega_{\text{ex}}$ is the detuning, and g_c represents the coupling strength. A fit to the UPB and LPB peak energies using the JC model is shown in Figure 4a,c. As we can see, the errors of peak energies between different group of spectra are very small, showing the high robustness and reproducibility of the coupled system. The JC model fits to the peak energies show a Rabi splitting ($\Omega = 2g_c|_{\delta=0}$) of about 110 meV for eight-layer devices, which satisfies the criterion for strong coupling ($\Omega > (\Gamma_{\text{pl}} + \Gamma_{\text{ex}})/2$). However, the Rabi splitting for the single-layer device is approximately 80 meV, indicating that the system is in intermediate-coupling regime ($\Omega > (\Gamma_{\text{pl}} - \Gamma_{\text{ex}})/2$).⁵⁹ Numerical calculations provide another piece of evidence for our observations. By modeling the excitonic dielectric permittivity of the MoS₂ as a Lorentz oscillator, we calculated the scattering cross section of hybrid structures with changes in the gap distance from 20 to 50 nm (Figure 4b,d), showing an anticrossing of two normal modes.

On comparison with the calculated results, the intensity of UPBs in experiments always seems to be lower than that of LPBs, which could be due to the rapid attenuation of the gap mode with an increase in the gap and the non-negligible emission of uncoupled A excitons outside the nanocavity. The JC model fits and calculations also reveal the moderate anticrossing behavior of UPBs and LPBs in Figure 4a,c. Due to the small tuning range of the plasmon mode with increasing

gap sizes and the strong coupling of excitons and plasmons optimized to near resonance, the energies of UPBs and LPBs move more slowly in comparison with that of the plasmon mode during the tuning process, making the data points look horizontal and less curved. Additionally, the small number of excitons contributing to the coupling with the gap mode also accounts for the mismatch between JC model fits and plexciton branches because of the strong background signal. For example, the emission of massive uncoupled excitons near bowties in scattering spectra will affect the extraction of plexciton branches.

To evaluate the exciton number evolved in the strong coupling, we use $g_c = \sqrt{N}\boldsymbol{\mu}\cdot\mathbf{E}_{\text{vac}} = \sqrt{N}\boldsymbol{\mu}\cdot\mathbf{E}_{\text{vac}}|\mathbf{K}$, where N is the effective exciton number coherently contributing to the interaction with the cavity, $\boldsymbol{\mu}$ is exciton transition dipole moment, $|\mathbf{E}_{\text{vac}}| = \sqrt{\hbar\omega/2\epsilon_r\epsilon_0V_m}$ is the vacuum field amplitude,^{14,60} and \mathbf{K} is unit vector, satisfying $|\mathbf{K}| = 1$. Because the exciton dipole strength in TMDs is highly anisotropic^{52,61} and has an out-of-plane component in multiple layers, the coupling strength can be written as

$$g_c = \sqrt{N}|\mathbf{E}_{\text{vac}}|(\boldsymbol{\mu}_{xy} + \boldsymbol{\mu}_z)\cdot(\mathbf{K}_{xy} + \mathbf{K}_z) \quad (2)$$

where $\boldsymbol{\mu}_{xy}$ and $\boldsymbol{\mu}_z$ represent the in-plane and out-of-plane dipole moments, respectively, and $\mathbf{K} = \mathbf{K}_{xy} + \mathbf{K}_z$ with \mathbf{K}_{xy} being parallel to the two-dimensional semiconductors plane and \mathbf{K}_z being perpendicular to the plane. Therefore, the coupling strength can be expressed as a form of contribution from in-plane and out-of-plane dipole moments: $g_c = \sqrt{N}|\mathbf{E}_{\text{vac}}|(\mu_{xy}K_{xy} + \mu_zK_z)$. Here, we define the ratio of in-plane field as $\beta_{xy} = |\mathbf{K}_{xy}|^2$, which represents the ratio of an

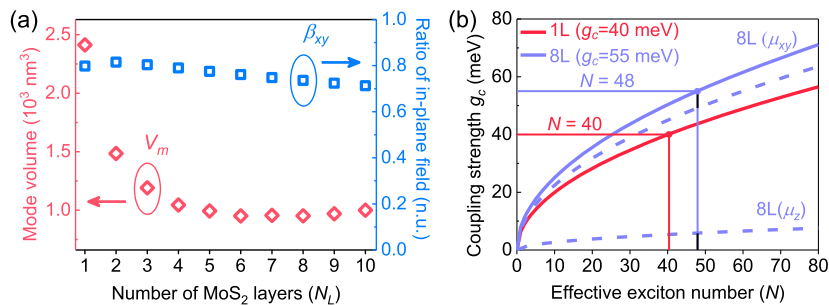


Figure 5. Effective exciton number of the coupled system. (a) Mode volume V_m and ratio of in-plane field β_{xy} as a function of the number of MoS₂ layers with the same gap distance of about 20 nm. (b) Coupling strength g_c as a function of the effective exciton number (N) for single-layer and eight-layer systems. The dashed blue lines show the in-plane (μ_{xy}) and out-of-plane (μ_z) coupling strength components.

Table 1. Reported Effective Exciton Numbers in Different Plasmonic Cavities

structure	material	Ω (meV)	N (μ_0^a (D))	N (μ_{qw}^a (D))	N (μ_{ab}^a (D))
single gold nanoprism on gold film (gap plasmon) ³⁵	WS ₂	76	2 (56)	111 (7.53)	198 (5.63)
single gold dimer (gap plasmon) ⁴⁹	WS ₂	115.2–128.6	4.67–7.69 (56)	258–425 (7.53)	462–761 (5.63)
single silver nanocube on silver film (gap plasmon) ³⁶	WS ₂	145	130 (56)	7190 (7.53)	12862 (5.63)
silver nanoparticle array ⁴⁸	WS ₂	52	3000 (50)	~132000 (7.53)	~236000 (5.63)
single silver nanorod ³³	WSe ₂	49.5	4100 (7.67)		
single gold nanorod ⁴³	WS ₂	106	~12	225 (7.53)	403 (5.63)
our work: single gold bowtie (gap plasmon)	MoS ₂	80–110		38 (7.51)	40 (7.36), 48 (8 layer)

^a μ_0 is the transition dipole moment in the references cited, μ_{qw} is the corrected transition dipole moment with the quantum well model, and μ_{ab} is calculated with absorption spectra.

integral of in-plane field components to the total electric field and can be numerically calculated by

$$\beta_{xy} = \int_{V_e} \frac{E_x^2 + E_y^2}{E_x^2 + E_y^2 + E_z^2} dV_e \quad (3)$$

where V_e represents the volume of the excitonic material. Similarly, we can get the ratio of out-of-plane field β_z with $\beta_{xy} + \beta_z = 1$. Finally, the coupling strength can be written as

$$g_c = \sqrt{\frac{N\hbar\omega}{2\epsilon_r\epsilon_0V_m}} (\mu_{xy}\sqrt{\beta_{xy}} + \mu_z\sqrt{\beta_z}) \quad (4)$$

Figure 5a shows the mode volumes as a function of the layer number. The mode volume of the bowtie nanocavity is about 10^3 nm³ for a single layer, which is comparable to the current optimal results for single nanoparticles such as gold bipyramids³⁴ or ultrasmall gold nanorods⁴³ and is even smaller in the case with multiple layer coverage. With an increase in the layer number, the mode volume gradually decreases from 2413 to 951 nm³ and then saturates. This means that the electric field is strengthened and is more tightly confined in TMD layers, which explains why larger splittings are observed in multiple layers. The ratio of an integral of the in-plane field to the total field is about 71–80% in different layers, as shown in Figure 5a, confirming that the dominant electric field component of the gap plasmon in our system is the in-plane component E_{xy} .

In order to estimate the number of excitons involved in coupling, the transition dipole moment of the excitons in a TMD layer is another significant parameter. Here, we adopt two methods, i.e. the quantum well method and absorbance measurements, to estimate this value. The quantum well method regards the 2D TMD layers as quantum-well structures similar to III–V semiconductors⁵⁰ and takes into account that the electron of TMDs has a large effective mass

m_c around the K point, giving $\mu = \frac{e\hbar}{2E_0} \left[\frac{E_g(E_g + \Delta_0)}{E_g + 2\Delta_0/3} \left(\frac{1}{m_c} - \frac{1}{m_0} \right) \right]^{1/2}$

, where E_0 is the transition energy of the exciton, E_g is the band gap, and Δ_0 is the spin–orbit splitting in the valence band. The absorbance measurements consider the relationship between the 2D susceptibility of excitons with a 1s hydrogen-like wave function and absorption A_{ex}^{2D} of the thin layer,^{33,62} giving

$A_{ex}^{2D} = \frac{4\eta_0\omega_{ex}}{\pi a_B^2 \Gamma_{ex}} \mu^2$, where η_0 is the free space impedance, a_B is the Bohr radius of an exciton, and ω_{ex} and Γ_{ex} are the energy and line width of an exciton, respectively. Both methods give similar dipole moment values for TMD layers, such as 7.53 and 5.63 D for monolayer WS₂ and 7.51 and 7.36 D for monolayer MoS₂, respectively (see Section III of the Supporting Information for more details). It should be noted that our calculation result is much smaller than the value of 56 D reported in the literature,⁶³ where the reduced Planck constant (\hbar) should have been used, as discussed in the Supporting Information. For the case of several layers, we determined the in-plane dipole moment using $\mu_{xy} \propto \sqrt{abs}$, where abs is spectrally integrated for the A excitonic transition.⁴⁸ Using the value of a single layer, we obtain the in-plane dipole moment $\mu_{xy}^{sl} \approx 5.07$ D and out-of-plane dipole moment $\mu_z^{sl} \approx 1.01$ D.

Figure 5b shows the calculated coupling strength g_c as a function of the effective exciton number N for a single layer and eight layers at resonance. We found that the effective exciton number is compressed down to $N \approx 40$ for the case of a single layer and $N \approx 48$ in multiple layers, indicating a small exciton number in such a coupling system with plasmon modes and excitons in two-dimensional semiconductors. Table 1 gives a comparison of the coupled systems with a small exciton number with those of some previous reports, in which the exciton numbers with corrected dipole moments are also included (see Section III of the Supporting Information for

more details). The effective exciton numbers are much larger with a corrected dipole moment in comparison with those reported.^{35,36,48,49} The numbers involved in a single-nanorod structure⁴³ are recalculated by the formula $g_c = \sqrt{N} \boldsymbol{\mu} \cdot \mathbf{E}_{\text{vac}}$ at zero tuning. The calculated exciton numbers are also much larger than those claimed. The small number of excitons in our experiment also explains the mismatch between JC model fitting and experimental results in Figure 4a,c due to the influence of emission of massive uncoupled excitons in layers around the bowtie. For multiple layers, the contribution to coupling strength is only 12% ($\mu_z \sqrt{\beta_z} / \mu_{xy} \sqrt{\beta_{xy}}$) of the in-plane component as shown in Figure 5b, indicating a selective coupling between the larger in-plane exciton dipole moment and the dominant in-plane field of the gap mode in our configuration as designed. Furthermore, the effective number in our system can be reduced more by further reducing the gap distance of the bowtie until it is comparable to the exciton coherence length (~ 4 nm). When the gap size is smaller than the exciton coherence length, the out-of-plane component of the gap mode located in the two tips of the bowtie will drive the exciton dipole with an opposite phase, as shown in Figure 1c, which prevents a further enhancement of coupling.

CONCLUSION

In summary, we have demonstrated a strong plasmon–exciton coupling between individual bowtie resonators and MoS₂ layers, with the effective exciton number contributing to the coupling down to 40 in a single layer and 48 in a few layers. Such a small exciton number in the plexciton system gives an opportunity to study the interaction between cavity and many emitters and to potentially achieve a strong coupling between a single exciton and plasmon in two-dimensional materials with a small mode volume.⁶⁴ Moreover, we have also demonstrated a universal method to obtain robust and reproducible plasmon–exciton interaction by utilizing a gold-assisted mechanical exfoliation method and wet transfer techniques, which paves the way to integrate the plexciton system into photonic devices and exploit novel quantum and nonlinear optical effects at room temperature.

ASSOCIATED CONTENT

Supporting Information

The Supporting Information is available free of charge at <https://pubs.acs.org/doi/10.1021/acs.nanolett.1c03282>.

Sample fabrication and characterizations, simulation and optimization of the plasmon mode in nanocavities, calculation of effective exciton numbers, and extra data of DF scattering spectra of coupled structures with single-layer and eight-layer MoS₂ (PDF)

AUTHOR INFORMATION

Corresponding Authors

Jianing Chen – Beijing National Laboratory for Condensed Matter Physics, Institute of Physics, Chinese Academy of Sciences, Beijing 100190, People's Republic of China; CAS Center for Excellence in Topological Quantum Computation and School of Physical Sciences, University of Chinese Academy of Sciences, Beijing 100049, People's Republic of China; Songshan Lake Materials Laboratory, Dongguan, Guangdong 523808, People's Republic of China; Email: jnchen@iphy.ac.cn

Yuan Huang – Beijing National Laboratory for Condensed Matter Physics, Institute of Physics, Chinese Academy of Sciences, Beijing 100190, People's Republic of China; CAS Center for Excellence in Topological Quantum Computation and School of Physical Sciences, University of Chinese Academy of Sciences, Beijing 100049, People's Republic of China; Songshan Lake Materials Laboratory, Dongguan, Guangdong 523808, People's Republic of China; Email: yhuang01@iphy.ac.cn

Can Wang – Beijing National Laboratory for Condensed Matter Physics, Institute of Physics, Chinese Academy of Sciences, Beijing 100190, People's Republic of China; CAS Center for Excellence in Topological Quantum Computation and School of Physical Sciences, University of Chinese Academy of Sciences, Beijing 100049, People's Republic of China; Songshan Lake Materials Laboratory, Dongguan, Guangdong 523808, People's Republic of China; orcid.org/0000-0002-4404-7957; Email: canwang@iphy.ac.cn

Xiulai Xu – Beijing National Laboratory for Condensed Matter Physics, Institute of Physics, Chinese Academy of Sciences, Beijing 100190, People's Republic of China; CAS Center for Excellence in Topological Quantum Computation and School of Physical Sciences, University of Chinese Academy of Sciences, Beijing 100049, People's Republic of China; Songshan Lake Materials Laboratory, Dongguan, Guangdong 523808, People's Republic of China; orcid.org/0000-0001-8231-406X; Email: xlxu@iphy.ac.cn

Authors

Longlong Yang – Beijing National Laboratory for Condensed Matter Physics, Institute of Physics, Chinese Academy of Sciences, Beijing 100190, People's Republic of China; CAS Center for Excellence in Topological Quantum Computation and School of Physical Sciences, University of Chinese Academy of Sciences, Beijing 100049, People's Republic of China

Xin Xie – Beijing National Laboratory for Condensed Matter Physics, Institute of Physics, Chinese Academy of Sciences, Beijing 100190, People's Republic of China; CAS Center for Excellence in Topological Quantum Computation and School of Physical Sciences, University of Chinese Academy of Sciences, Beijing 100049, People's Republic of China

Jingnan Yang – Beijing National Laboratory for Condensed Matter Physics, Institute of Physics, Chinese Academy of Sciences, Beijing 100190, People's Republic of China; CAS Center for Excellence in Topological Quantum Computation and School of Physical Sciences, University of Chinese Academy of Sciences, Beijing 100049, People's Republic of China

Mengfei Xue – Beijing National Laboratory for Condensed Matter Physics, Institute of Physics, Chinese Academy of Sciences, Beijing 100190, People's Republic of China; CAS Center for Excellence in Topological Quantum Computation and School of Physical Sciences, University of Chinese Academy of Sciences, Beijing 100049, People's Republic of China

Shiyao Wu – Beijing National Laboratory for Condensed Matter Physics, Institute of Physics, Chinese Academy of Sciences, Beijing 100190, People's Republic of China; CAS Center for Excellence in Topological Quantum Computation and School of Physical Sciences, University of Chinese

Academy of Sciences, Beijing 100049, People's Republic of China

Shan Xiao – Beijing National Laboratory for Condensed Matter Physics, Institute of Physics, Chinese Academy of Sciences, Beijing 100190, People's Republic of China; CAS Center for Excellence in Topological Quantum Computation and School of Physical Sciences, University of Chinese Academy of Sciences, Beijing 100049, People's Republic of China

Feilong Song – Beijing National Laboratory for Condensed Matter Physics, Institute of Physics, Chinese Academy of Sciences, Beijing 100190, People's Republic of China; CAS Center for Excellence in Topological Quantum Computation and School of Physical Sciences, University of Chinese Academy of Sciences, Beijing 100049, People's Republic of China

Jianchen Dang – Beijing National Laboratory for Condensed Matter Physics, Institute of Physics, Chinese Academy of Sciences, Beijing 100190, People's Republic of China; CAS Center for Excellence in Topological Quantum Computation and School of Physical Sciences, University of Chinese Academy of Sciences, Beijing 100049, People's Republic of China

Sibai Sun – Beijing National Laboratory for Condensed Matter Physics, Institute of Physics, Chinese Academy of Sciences, Beijing 100190, People's Republic of China; CAS Center for Excellence in Topological Quantum Computation and School of Physical Sciences, University of Chinese Academy of Sciences, Beijing 100049, People's Republic of China

Zhanchun Zuo – Beijing National Laboratory for Condensed Matter Physics, Institute of Physics, Chinese Academy of Sciences, Beijing 100190, People's Republic of China; CAS Center for Excellence in Topological Quantum Computation and School of Physical Sciences, University of Chinese Academy of Sciences, Beijing 100049, People's Republic of China

Xingjiang Zhou – Beijing National Laboratory for Condensed Matter Physics, Institute of Physics, Chinese Academy of Sciences, Beijing 100190, People's Republic of China; CAS Center for Excellence in Topological Quantum Computation and School of Physical Sciences, University of Chinese Academy of Sciences, Beijing 100049, People's Republic of China; Songshan Lake Materials Laboratory, Dongguan, Guangdong 523808, People's Republic of China

Kuijuan Jin – Beijing National Laboratory for Condensed Matter Physics, Institute of Physics, Chinese Academy of Sciences, Beijing 100190, People's Republic of China; CAS Center for Excellence in Topological Quantum Computation and School of Physical Sciences, University of Chinese Academy of Sciences, Beijing 100049, People's Republic of China; Songshan Lake Materials Laboratory, Dongguan, Guangdong 523808, People's Republic of China;

orcid.org/0000-0002-0047-4375

Complete contact information is available at:

<https://pubs.acs.org/10.1021/acs.nanolett.1c03282>

Notes

The authors declare no competing financial interest.

ACKNOWLEDGMENTS

This work was supported by the National Key Research and Development Program of China (Grant Nos. 2021YFA1400700, 2019YFA0308000, and 2018YFA0704201), the National Natural Science Foundation of China (Grant Nos. 62025507, 11934019, 11721404, 11874419, 11874405, 62022089, 62175254 and 12174437), the Key-Area Research and Development Program of Guangdong Province (Grant No. 2018B030329001), the Strategic Priority Research Program (Grant Nos. XDB28000000 and XDB33000000), the Youth Innovation Promotion Association of CAS (2019007) of the Chinese Academy of Sciences, and Chongqing Outstanding Youth Fund (Grant No. 2021ZX0400005). We thank Professor Masahiro Asada for helpful discussions.

REFERENCES

- (1) Chakraborty, C.; Kinnischtzke, L.; Goodfellow, K. M.; Beams, R.; Vamivakas, A. N. Voltage-controlled quantum light from an atomically thin semiconductor. *Nat. Nanotechnol.* **2015**, *10*, 507–511.
- (2) Dang, J.; Sun, S.; Xie, X.; Yu, Y.; Peng, K.; Qian, C.; Wu, S.; Song, F.; Yang, J.; Xiao, S.; Yang, L.; Wang, Y. W.; Rafiq, M. A.; Wang, C.; Xu, X. Identifying defect-related quantum emitters in monolayer WSe₂. *npj 2D Mater. Appl.* **2020**, *4*, 2.
- (3) Zhang, Y.; Ye, J.; Matsushashi, Y.; Iwasa, Y. Ambipolar MoS₂ thin flake transistors. *Nano Lett.* **2012**, *12*, 1136–1140.
- (4) Radisavljevic, B.; Radenovic, A.; Brivio, J.; Giacometti, V.; Kis, A. Single-layer MoS₂ transistors. *Nat. Nanotechnol.* **2011**, *6*, 147–150.
- (5) Mak, K. F.; McGill, K. L.; Park, J.; McEuen, P. L. The valley Hall effect in MoS₂ transistors. *Science* **2014**, *344*, 1489–1492.
- (6) Lopez-Sanchez, O.; Lembke, D.; Kayci, M.; Radenovic, A.; Kis, A. Ultrasensitive photodetectors based on monolayer MoS₂. *Nat. Nanotechnol.* **2013**, *8*, 497–501.
- (7) Xiao, D.; Liu, G.-B.; Feng, W.; Xu, X.; Yao, W. Coupled spin and valley physics in monolayers of MoS₂ and other group-VI dichalcogenides. *Phys. Rev. Lett.* **2012**, *108*, 196802.
- (8) Cao, T.; Wang, G.; Han, W.; Ye, H.; Zhu, C.; Shi, J.; Niu, Q.; Tan, P.; Wang, E.; Liu, B.; Feng, J. Valley-selective circular dichroism of monolayer molybdenum disulphide. *Nat. Commun.* **2012**, *3*, 887.
- (9) Ugeda, M. M.; Bradley, A. J.; Shi, S.-F.; da Jornada, F. H.; Zhang, Y.; Qiu, D. Y.; Ruan, W.; Mo, S.-K.; Hussain, Z.; Shen, Z.-X.; Wang, F.; Louie, S. G.; Crommie, M. F. Giant bandgap renormalization and excitonic effects in a monolayer transition metal dichalcogenide semiconductor. *Nat. Mater.* **2014**, *13*, 1091–1095.
- (10) He, K.; Kumar, N.; Zhao, L.; Wang, Z.; Mak, K. F.; Zhao, H.; Shan, J. Tightly bound excitons in monolayer WSe₂. *Phys. Rev. Lett.* **2014**, *113*, No. 026803.
- (11) Lundt, N.; Klemmt, S.; Cherotchenko, E.; Betzold, S.; Iff, O.; Nalitov, A. V.; Klaas, M.; Dietrich, C. P.; Kavokin, A. V.; Höfling, S.; Schneider, C. Room-temperature Tamm-plasmon exciton-polaritons with a WSe₂ monolayer. *Nat. Commun.* **2016**, *7*, 13328.
- (12) Wang, Z.; Dong, Z.; Gu, Y.; Chang, Y.-H.; Zhang, L.; Li, L.-J.; Zhao, W.; Eda, G.; Zhang, W.; Grinblat, G.; Maier, S. A.; Yang, J. K. W.; Qiu, C.-W.; Wee, A. T. S. Giant photoluminescence enhancement in tungsten-diselenide-gold plasmonic hybrid structures. *Nat. Commun.* **2016**, *7*, 11283.
- (13) Liu, X.; Galfsky, T.; Sun, Z.; Xia, F.; Lin, E.-c.; Lee, Y.-H.; Kéna-Cohen, S.; Menon, V. M. Strong light-matter coupling in two-dimensional atomic crystals. *Nat. Photonics* **2015**, *9*, 30–34.
- (14) Törmä, P.; Barnes, W. L. Strong coupling between surface plasmon polaritons and emitters: a review. *Rep. Prog. Phys.* **2015**, *78*, No. 013901.
- (15) Deng, H.; Weihs, G.; Santori, C.; Bloch, J.; Yamamoto, Y. Condensation of semiconductor microcavity exciton polaritons. *Science* **2002**, *298*, 199–202.
- (16) Kasprzak, J.; Richard, M.; Baas, A.; Jeambrun, P.; Keeling, J. M. J.; Marchetti, F. M.; Szymańska, M. H.; André, R.

- Staepli, J. L.; Savona, V.; Littlewood, P. B.; Deveaud, B.; Dang, L. S. Bose–Einstein condensation of exciton polaritons. *Nature* **2006**, *443*, 409–414.
- (17) Christopoulos, S.; Von Högersthal, G. B. H.; Grundy, A. J. D.; Lagoudakis, P. G.; Kavokin, A. V.; Baumberg, J. J.; Christmann, G.; Butté, R.; Feltn, E.; Carlin, J.-F.; Grandjean, N. Room-temperature polariton lasing in semiconductor microcavities. *Phys. Rev. Lett.* **2007**, *98*, 126405.
- (18) Kéna-Cohen, S.; Forrest, S. R. Room-temperature polariton lasing in an organic single-crystal microcavity. *Nat. Photonics* **2010**, *4*, 371.
- (19) Dreismann, A.; Ohadi, H.; Redondo, Y. d. V.-I.; Balili, R.; Rubo, Y. G.; Tsintzos, S. I.; Deligeorgis, G.; Hatzopoulos, Z.; Savvidis, P. G.; Baumberg, J. J. A sub-femtojoule electrical spin-switch based on optically trapped polariton condensates. *Nat. Mater.* **2016**, *15*, 1074–1078.
- (20) Ballarini, D.; De Giorgi, M.; Cancellieri, E.; Houdré, R.; Giacobino, E.; Cingolani, R.; Bramati, A.; Gigli, G.; Sanvitto, D. All-optical polariton transistor. *Nat. Commun.* **2013**, *4*, 1778.
- (21) Wallraff, A.; Schuster, D. I.; Blais, A.; Frunzio, L.; Huang, R.-S.; Majer, J.; Kumar, S.; Girvin, S. M.; Schoelkopf, R. J. Strong coupling of a single photon to a superconducting qubit using circuit quantum electrodynamics. *Nature* **2004**, *431*, 162–167.
- (22) Amo, A.; Liew, T. C. H.; Adrados, C.; Houdré, R.; Giacobino, E.; Kavokin, A. V.; Bramati, A. Exciton-polariton spin switches. *Nat. Photonics* **2010**, *4*, 361–366.
- (23) Xie, X.; Zhang, W.; He, X.; Wu, S.; Dang, J.; Peng, K.; Song, F.; Yang, L.; Ni, H.; Niu, Z.; Wang, C.; Jin, K.; Zhang, X.; Xu, X. Cavity Quantum Electrodynamics with Second-Order Topological Corner State. *Laser & Photonics Reviews* **2020**, *14*, 1900425.
- (24) Qian, C.; Xie, X.; Yang, J.; Peng, K.; Wu, S.; Song, F.; Sun, S.; Dang, J.; Yu, Y.; Steer, M. J.; Thayne, I. G.; Jin, K.; Gu, C.; Xu, X. Enhanced Strong Interaction between Nanocavities and *p*-shell Excitons Beyond the Dipole Approximation. *Phys. Rev. Lett.* **2019**, *122*, No. 087401.
- (25) Dufferwiel, S.; et al. Exciton-polaritons in van der Waals heterostructures embedded in tunable microcavities. *Nat. Commun.* **2015**, *6*, 8579.
- (26) Chen, Y.-J.; Cain, J. D.; Stanev, T. K.; Dravid, V. P.; Stern, N. P. Valley-polarized exciton–polaritons in a monolayer semiconductor. *Nat. Photonics* **2017**, *11*, 431–435.
- (27) Zhang, L.; Gogna, R.; Burg, W.; Tutuc, E.; Deng, H. Photonic-crystal exciton-polaritons in monolayer semiconductors. *Nat. Commun.* **2018**, *9*, 713.
- (28) Flatten, L. C.; He, Z.; Coles, D. M.; Trichet, A. A. P.; Powell, A. W.; Taylor, R. A.; Warner, J. H.; Smith, J. M. Room-temperature exciton-polaritons with two-dimensional WS₂. *Sci. Rep.* **2016**, *6*, 33134.
- (29) Kleemann, M.-E.; Chikkaraddy, R.; Alexeev, E. M.; Kos, D.; Carnegie, C.; Deacon, W.; de Pury, A. C.; Große, C.; de Nijs, B.; Mertens, J.; Tartakovskii, A. I.; Baumberg, J. J. Strong-coupling of WS₂ in ultra-compact plasmonic nanocavities at room temperature. *Nat. Commun.* **2017**, *8*, 1296.
- (30) Hu, F.; Fei, Z. Recent Progress on Exciton Polaritons in Layered Transition-Metal Dichalcogenides. *Advanced Optical Materials* **2020**, *8*, 1901003.
- (31) Chikkaraddy, R.; de Nijs, B.; Benz, F.; Barrow, S. J.; Scherman, O. A.; Rosta, E.; Demetriadou, A.; Fox, P.; Hess, O.; Baumberg, J. J. Single-molecule strong coupling at room temperature in plasmonic nanocavities. *Nature* **2016**, *535*, 127–130.
- (32) Santhosh, K.; Bitton, O.; Chuntunov, L.; Haran, G. Vacuum Rabi splitting in a plasmonic cavity at the single quantum emitter limit. *Nat. Commun.* **2016**, *7*, 11823.
- (33) Zheng, D.; Zhang, S.; Deng, Q.; Kang, M.; Nordlander, P.; Xu, H. Manipulating coherent plasmon–exciton interaction in a single silver nanorod on monolayer WS₂. *Nano Lett.* **2017**, *17*, 3809–3814.
- (34) Stührenberg, M.; Munkhbat, B.; Baranov, D. G.; Cuadra, J.; Yankovich, A. B.; Antosiewicz, T. J.; Olsson, E.; Shegai, T. Strong light–matter coupling between plasmons in individual gold bi-pyramids and excitons in mono- and multilayer WS₂. *Nano Lett.* **2018**, *18*, 5938–5945.
- (35) Qin, J.; Chen, Y.-H.; Zhang, Z.; Zhang, Y.; Blaikie, R. J.; Ding, B.; Qiu, M. Revealing Strong Plasmon-Exciton Coupling between Nanogap Resonators and Two-Dimensional Semiconductors at Ambient Conditions. *Phys. Rev. Lett.* **2020**, *124*, No. 063902.
- (36) Han, X.; Wang, K.; Xing, X.; Wang, M.; Lu, P. Rabi Splitting in a Plasmonic Nanocavity Coupled to a WS₂ Monolayer at Room Temperature. *ACS Photonics* **2018**, *5*, 3970–3976.
- (37) Hartmann, M. J.; Brandao, F. G.; Plenio, M. B. Quantum many-body phenomena in coupled cavity arrays. *Laser & Photonics Reviews* **2008**, *2*, 527–556.
- (38) Trivedi, R.; Radulaski, M.; Fischer, K. A.; Fan, S.; Vučković, J. Photon blockade in weakly driven cavity quantum electrodynamics systems with many emitters. *Phys. Rev. Lett.* **2019**, *122*, 243602.
- (39) Hosseini, M.; Duan, Y.; Beck, K. M.; Chen, Y.-T.; Vuletić, V. Cavity cooling of many atoms. *Phys. Rev. Lett.* **2017**, *118*, 183601.
- (40) Hennessy, K.; Badolato, A.; Winger, M.; Gerace, D.; Atature, M.; Gulde, S.; Fält, S.; Hu, E. L.; Imamoglu, A. Quantum nature of a strongly coupled single quantum dot–cavity system. *Nature* **2007**, *445*, 896–899.
- (41) Faraon, A.; Fushman, I.; Englund, D.; Stoltz, N.; Petroff, P.; Vučković, J. Coherent generation of non-classical light on a chip via photon-induced tunnelling and blockade. *Nat. Phys.* **2008**, *4*, 859–863.
- (42) Qi, X.; Lo, T. W.; Liu, D.; Feng, L.; Chen, Y.; Wu, Y.; Ren, H.; Guo, G.-C.; Lei, D.; Ren, X. Effects of gap thickness and emitter location on the photoluminescence enhancement of monolayer MoS₂ in a plasmonic nanoparticle-film coupled system. *Nanophotonics* **2020**, *9*, 2097–2105.
- (43) Wen, J.; Wang, H.; Wang, W.; Deng, Z.; Zhuang, C.; Zhang, Y.; Liu, F.; She, J.; Chen, J.; Chen, H.; Deng, S.; Xu, N. Room-Temperature Strong Light-Matter Interaction with Active Control in Single Plasmonic Nanorod Coupled with Two-Dimensional Atomic Crystals. *Nano Lett.* **2017**, *17*, 4689–4697.
- (44) Geisler, M.; Cui, X.; Wang, J.; Rindzevicius, T.; Gammelgaard, L.; Jessen, B. S.; Gonçalves, P. A. D.; Todisco, F.; Bøggild, P.; Boisen, A.; Wubs, M.; Mortensen, N. A.; Xiao, S.; Stenger, N. Single-Crystalline Gold Nanodisks on WS₂ Mono- and Multilayers for Strong Coupling at Room Temperature. *ACS Photonics* **2019**, *6*, 994–1001.
- (45) Lo, T. W.; Zhang, Q.; Qiu, M.; Guo, X.; Meng, Y.; Zhu, Y.; Xiao, J. J.; Jin, W.; Leung, C. W.; Lei, D. Thermal Redistribution of Exciton Population in Monolayer Transition Metal Dichalcogenides Probed with Plasmon–Exciton Coupling Spectroscopy. *ACS Photonics* **2019**, *6*, 411–421.
- (46) Liu, R.; Zhou, Z.-K.; Yu, Y.-C.; Zhang, T.; Wang, H.; Liu, G.; Wei, Y.; Chen, H.; Wang, X.-H. Strong light-matter interactions in single open plasmonic nanocavities at the quantum optics limit. *Phys. Rev. Lett.* **2017**, *118*, 237401.
- (47) Tame, M. S.; McEneaney, K. R.; Özdemir, Ş. K.; Lee, J.; Maier, S. A.; Kim, M. S. Quantum plasmonics. *Nat. Phys.* **2013**, *9*, 329–340.
- (48) Wang, S.; Le-Van, Q.; Vaianella, F.; Maes, B.; Eizagirre Barker, S.; Godiksen, R. H.; Curto, A. G.; Gomez Rivas, J. Limits to strong coupling of excitons in multilayer WS₂ with collective plasmonic resonances. *ACS Photonics* **2019**, *6*, 286–293.
- (49) Liu, L.; Tobing, L. Y.; Wu, T.; Qiang, B.; Garcia-Vidal, F. J.; Zhang, D. H.; Wang, Q. J.; Luo, Y. Plasmon-induced thermal tuning of few-exciton strong coupling in 2D atomic crystals. *Optica* **2021**, *8*, 1416–1423.
- (50) Asada, M.; Kameyama, A.; Suematsu, Y. Gain and intervalence band absorption in quantum-well lasers. *IEEE Journal of Quantum Electronics* **1984**, *20*, 745–753.
- (51) Lee, B.; Park, J.; Han, G. H.; Ee, H.-S.; Naylor, C. H.; Liu, W.; Johnson, A. T. C.; Agarwal, R. Fano resonance and spectrally modified photoluminescence enhancement in monolayer MoS₂ integrated with plasmonic nanoantenna array. *Nano Lett.* **2015**, *15*, 3646–3653.

(52) Schuller, J. A.; Karaveli, S.; Schiros, T.; He, K.; Yang, S.; Kyymissis, I.; Shan, J.; Zia, R. Orientation of luminescent excitons in layered nanomaterials. *Nat. Nanotechnol.* **2013**, *8*, 271–276.

(53) Baranov, D. G.; Wersäll, M.; Cuadra, J.; Antosiewicz, T. J.; Shegai, T. Novel nanostructures and materials for strong light–matter interactions. *ACS Photonics* **2018**, *5*, 24–42.

(54) Hartsfield, T.; Chang, W.-S.; Yang, S.-C.; Ma, T.; Shi, J.; Sun, L.; Shvets, G.; Link, S.; Li, X. Single quantum dot controls a plasmonic cavity's scattering and anisotropy. *Proc. Natl. Acad. Sci. U. S. A.* **2015**, *112*, 12288–12292.

(55) Yan, X.; Wei, H. Strong plasmon–exciton coupling between lithographically defined single metal nanoparticles and monolayer WSe₂. *Nanoscale* **2020**, *12*, 9708–9716.

(56) Huang, Y.; et al. Universal mechanical exfoliation of large-area 2D crystals. *Nat. Commun.* **2020**, *11*, 2453.

(57) Xu, G.; Tazawa, M.; Jin, P.; Nakao, S.; Yoshimura, K. Wavelength tuning of surface plasmon resonance using dielectric layers on silver island films. *Appl. Phys. Lett.* **2003**, *82*, 3811–3813.

(58) Qian, C.; Wu, S.; Song, F.; Peng, K.; Xie, X.; Yang, J.; Xiao, S.; Steer, M. J.; Thayne, I. G.; Tang, C.; Zuo, Z.; Jin, K.; Gu, C.; Xu, X. Two-Photon Rabi Splitting in a Coupled System of a Nanocavity and Exciton Complexes. *Phys. Rev. Lett.* **2018**, *120*, 213901.

(59) Leng, H.; Szychowski, B.; Daniel, M.-C.; Pelton, M. Strong coupling and induced transparency at room temperature with single quantum dots and gap plasmons. *Nat. Commun.* **2018**, *9*, 4012.

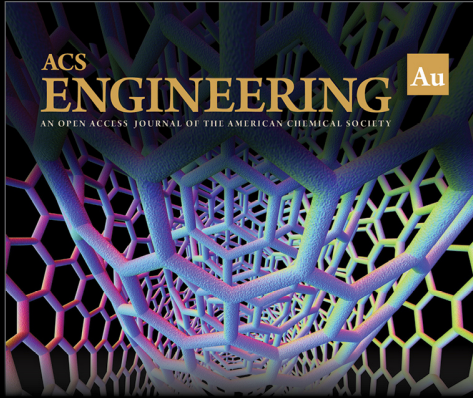
(60) Zengin, G.; Wersäll, M.; Nilsson, S.; Antosiewicz, T. J.; Käll, M.; Shegai, T. Realizing strong light-matter interactions between single-nanoparticle plasmons and molecular excitons at ambient conditions. *Phys. Rev. Lett.* **2015**, *114*, 157401.

(61) Liang, W. Y. Optical anisotropy in layer compounds. *J. Phys. C: Solid State Phys.* **1973**, *6*, 551.

(62) Vasilevskiy, M. I.; Santiago-Pérez, D. G.; Trallero-Giner, C.; Peres, N. M. R.; Kavokin, A. Exciton polaritons in two-dimensional dichalcogenide layers placed in a planar microcavity: Tunable interaction between two Bose–Einstein condensates. *Phys. Rev. B* **2015**, *92*, 245435.

(63) Sie, E. J.; Mciver, J. W.; Lee, Y. H.; Fu, L.; Kong, J.; Gedik, N. Valley-selective optical Stark effect in monolayer WS₂. *Nat. Mater.* **2015**, *14*, 290–294.


(64) Li, W.; Zhou, Q.; Zhang, P.; Chen, X.-W. Bright Optical Eigenmode of 1 nm³ Mode Volume. *Phys. Rev. Lett.* **2021**, *126*, 257401.




ACS
ENGINEERING Au
AN OPEN ACCESS JOURNAL OF THE AMERICAN CHEMICAL SOCIETY

Editor-in-Chief: **Prof. Shelley D. Minteer**, University of Utah, USA

Deputy Editor:
Prof. Vivek Ranade
University of Limerick, Ireland

Open for Submissions 

pubs.acs.org/engineeringau  ACS Publications
Most Trusted. Most Cited. Most Read.